25th ABCM International Congress of Mechanical Engineering
October 20-25, 2019, Uberlândia, MG, Brazil

COB-2019-0386
THREE-DIMENSIONAL LAMINAR SWIRLING FLOW IN A PIPE

Rodrigo Vidal Cabral
André Damiani Rocha
Energy Engineering Modeling and Simulation Laboratory (EEMSL)
Federal University of ABC, Av. dos Estados 5001 - Bangú - Santo André-SP
rodrigo.cabral@ufabc.edu.br, a.damiani@ufabc.edu.br

Abstract. *This paper presents the numerical flow field features of a three-dimensional laminar swirling flow in a pipe induced by static swirler guide vane-type. The numerical analysis has been carried using commercial computational fluid dynamics package* $Ansys^{®}$ *Fluent for axial Reynolds numbers less than 300. Along a 91.2 mm i.d. size and 2.7 m long pipe. The swirling flow is generated from a static swirler with 7 vanes, with deflection angle of 63.5 and gap width of 5 mm. Axial and tangential velocity components as well as swirl number along of pipe were computed. The results show that the helical flow is asymmetric, mainly in the region near the swirler. In addition, the results show that swirl decay is only exponential for* $Re \geq 200$*. The numerical results confirmed a helical nature to such kind of flows.*

Keywords: *swirling pipe flow, laminar swirling flow, static swirler*

1. INTRODUCTION

Swirl flow have wide range of applications in various engineering areas such as chemical and mechanical mixing and separation devices, combustion chambers, turbo machinery, fusion reactors, pollution control devices, etc. In nature, cyclone-type flows are commonly encountered in tidal currents at sea. A flow with swirl in pipe can be loosely defined as a motion combining an axial component of velocity with a tangential one. Typically, a fluid element in a such flow moves along helical paths, and regions of backflow may appear near of the axis of the pipe. One of the first studies on laminar swirling flow was carried out by (Talbot, 1951), through an analytical and experimental approach to low Reynolds numbers. He focused on the decay of the swirl superimposed onto a Poiseuille flow in a cylindrical duct, by solving a linearized equation for azimuthal velocity, and by treating the radial velocity and the axial deviation from the Poiseuille parabolic profile as perturbations. Other studies of viscous laminar swirling flow with stationary or rotating pipe were also performed (Lavan (1969), (Kiya *et al.*, 1970), (Singh *et al.*, 1980), (Silvester *et al.*, 1984)).

Considering low Reynolds numbers ($Re \leq 40$), the authors studied the axial velocity distribution, the decay of the swirl and discussed on flow instabilities which are known as vortex breakdown. (Ayinde, 2010) conducted numerical calculations on the three-dimensional laminar swirling flow in a pipe and a swirl decay rate correlation was proposed accounting the effects of the flow Reynolds number, the pipe length, inlet swirl intensity and the inlet swirl profile. (Rocha *et al.*, 2015) and (Rocha *et al.*, 2017) investigated the features of laminar swirling ($Re \leq 2000$) flow in a two-dimensional domain considering axisymmetric swirl flow. The effects of inlet boundary conditions and the influence of Reynolds number, deflection angle and gap width on fluid flow was investigated. The authors confirmed that the tangential velocity is a combination of forced and free vortex and small gap width and large deflection angle provides a larger swirl number. In addition, a correlation to predict the length of developed flow was proposed as a function of Reynolds number and swirl number at inlet.

The literature reveals the fact that, depending on the boundary conditions, swirling flows can undergo totally different scenarios and the flow field can exhibit different dynamical features. Most of the previously analytical or numerical studies of laminar swirling flow considered the two-dimensional flow with axial symmetry. In addition, the tangential component at inlet was considered like a combination of forced vortex in the core and free vortex in the annulus at inlet and the axial component was considering constant or a Poiseuille flow condition ((Kiya *et al.*, 1970), (Singh *et al.*, 1980), (Padmanabhan, 1984), (Benay, 1984); (Aksel and Kaya, 1992), (Shuja *et al.*, 2002), (Benim *et al.*, 2007), (Ayinde, 2010), (Yao and Fang, 2012), (Rocha *et al.*, 2015), (Beaubert *et al.*, 2016), (Rocha *et al.*, 2017)). Physically, the swirl flows can be generated using various swirl-generating methods. Commonly, the methods used to induce swirl in laminar flow are tangential entry such as axial-plus-tangential entry swirl generators (Bottaro *et al.*, 1991), guided vanes such as swirl vane packs, swirlers (Maynard, 2000), honeycomb structures (Vaidya *et al.*, 2011) and direct rotation such as rotating pipes

((Lavan, 1969), (Crane and Burley, 1976), (Silvester *et al.*, 1984), (Korjack, 1985)).

The purpose of this paper is to investigate flow field features of a laminar swirling flow in a pipe induced by static swirler guide vane-type. The full domain consists in an inlet fixed pipe, static guide vanes and outlet fixed pipe. Numerical analysis was carried out using $Ansys^{®}Fluent$ package and results of flow field and swirl decay are discussed.

2. SWIRLER

In order to generate the swirl, a guide vane-type is used. The geometry was designed by Cabral (Cabral and Rocha, 2017) and it is an enhanced swirler design from Rocha (Rocha, 2013). The swirler has been designed based on a deflection angle of 63.5 and consists in a spherical nose leading edge, an annulus section with 7 vanes and conical trailing edge. Figure 1 shows the swirler used in present work.

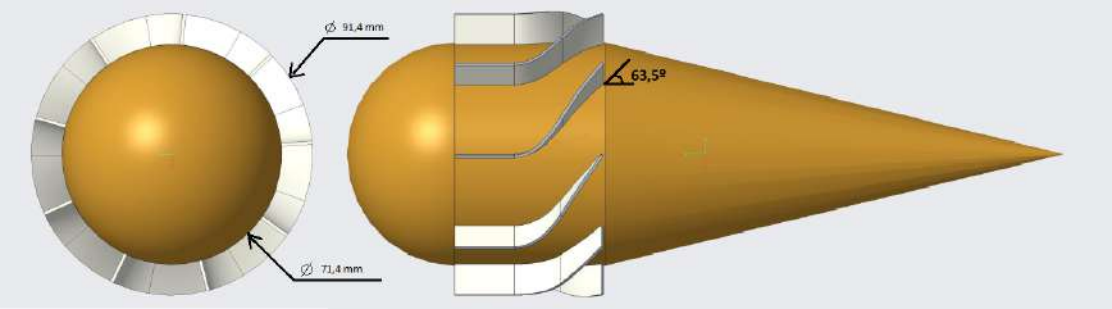

Figure 1. Swirler representation

3. NUMERICAL MODELING

The behavior of the flow is governed by the fundamental principles of classical fluid mechanics expressing the conservation of mass and momentum. As the flow is assumed to be isothermal steady laminar flow with constant properties, incompressible and three-dimensional. Neglecting gravitational effects, the reduced set of equations, in cylindrical coordinates (θ, r, z) with (u, v, w) velocity components, to be solved is then:

Equation of continuity

$$\frac{1}{r}\frac{\partial(rv)}{\partial r} + \frac{1}{r}\frac{\partial(u)}{\partial \theta} + \frac{\partial w}{\partial z} = 0 \tag{1}$$

Quantity of movement – radial direction (r)

$$\rho\left(v\frac{\partial v}{\partial r} + \frac{u}{r}\frac{\partial v}{\partial \theta} - \frac{u^2}{r} + w\frac{\partial v}{\partial z}\right) = -\frac{\partial p}{\partial r} + \mu\left\{\frac{\partial}{\partial r}\left[\frac{1}{r}\frac{\partial}{\partial r}(rv)\right] + \frac{1}{r^2}\frac{\partial^2 v}{\partial \theta^2} - \frac{2}{r^2}\frac{\partial u}{\partial \theta} + \frac{\partial^2 v}{\partial w^2}\right\} \tag{2}$$

Quantity of movement – tangential or circumferential direction (θ)

$$\rho\left(v\frac{\partial u}{\partial r} + \frac{u}{r}\frac{\partial u}{\partial \theta} + \frac{vu}{r} + w\frac{\partial u}{\partial z}\right) = -\frac{1}{r}\frac{\partial p}{\partial \theta}\mu\left\{\frac{\partial}{\partial r}\left[\frac{1}{r}\frac{\partial}{\partial r}(ru)\right] + \frac{1}{r^2}\frac{\partial^2 u}{\partial \theta^2} + \frac{2}{r^2}\frac{\partial v}{\partial \theta} + \frac{\partial^2 u}{\partial w^2}\right\} \tag{3}$$

Quantity of movement – axial direction (z)

$$\rho\left(v\frac{\partial w}{\partial r} + \frac{u}{r}\frac{\partial w}{\partial \theta} + w\frac{\partial w}{\partial z}\right) = -\frac{\partial p}{\partial z} + \mu\left\{\frac{1}{r}\frac{\partial}{\partial r}\left(r\frac{\partial w}{\partial r}\right) + \frac{1}{r^2}\frac{\partial^2 w}{\partial \theta^2} + \frac{\partial^2 w}{\partial z^2}\right\} \tag{4}$$

were ρ and μ are fluid density and fluid dynamic viscosity, respectively.

For engineering purposes, it is important to understand the decay process of swirl along the pipe. In order to estimate the effect of swirl, a swirl number S is introduced. The swirl number express the ratio of the axial flux of tangential momentum to the axial flux of axial momentum.

$$S = \frac{\int_0^R wur^2 dr}{R\int_0^R w^2 r dr} \tag{5}$$

where R is the hydraulic radius.

The equations (1-4) were solved using the finite volume technique embodied on the $Ansys^{®}Fluent$. The pressure-based solver with a Coupled, which as solves pressure and momentum simultaneously, was used. This algorithm is applicable for most single-phase flows and yields superior performance to the segregated solvers (Fluent, 2019). The second order upwind discretization scheme has been employed for pressure and momentum equations to ensure good accuracy. The computational convergence criteria are ensured when the residuals are lower than 10^{-6}. The flow domain is depicted in Fig. 2.

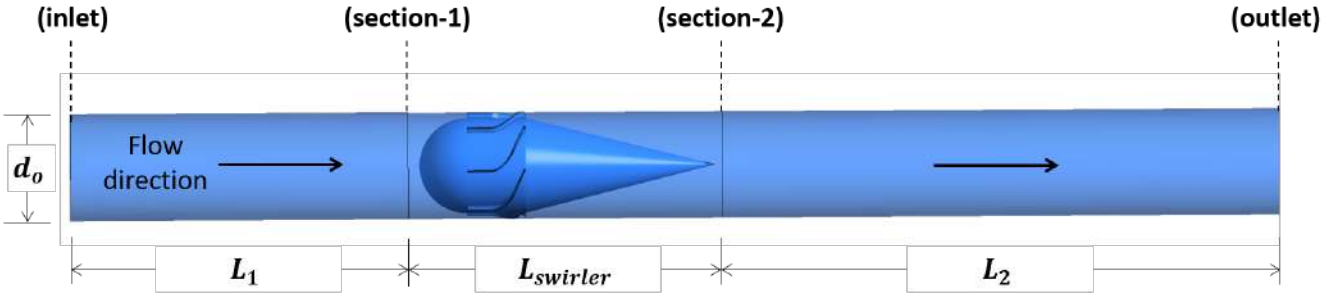

Figure 2. Computational domain

Boundary conditions must be specified in order to solve the governing equations. At the inlet, the mean axial velocity is specified and its is calculated as a function of Reynolds number defined by

$$Re = \frac{\rho v D}{\mu} \tag{6}$$

where ρ is density of fluid, v the average velocity of inlet, D the pipe diameter and μ the dynamic viscosity.

Table 1. Dimensions of computational domain, testing conditions and fluid properties.

Parameter	Quantity
1. Tube length (m)	2.77
2. Inner diameter (mm)	91.2
3. Deflection angle	$63,5°$
4. Working fluid	Water
5. Density @ 25°C (kg/m3)	998.2
6. Viscosity @ 25°C (Pa.s)	0.001
7. Reynolds number	25 - 300

At the outlet, there is no information about the variables and some assumptions must be made. The momentum diffusion fluxes in the direction normal to the exit plane are assumed to be zero. The pressure at the outlet boundary is specified. At the solids walls, the non-slip condition was applied.

Mesh generation is the most important task before performing any simulation. Adequately fine meshes are generated to ensure the accurate flow computation. In this work, tetrahedral mesh is generated by using $Ansys^{®}Meshing$ software. Fig. 3 shows the mesh at the swirler.

The grid independence test was carried out using the Grid Convergence Index (GCI) method (Roache, 1994; Celik, 2008), in which three meshes and generalized Richardson extrapolation are used to compute and report discretization errors. Three different grids and the three variables (axial velocity and tangential velocity at blade trailing edge and swirler pressure drop) were used to verify the independence of the results according to the grid refinements. Table 2 show the GCI results.

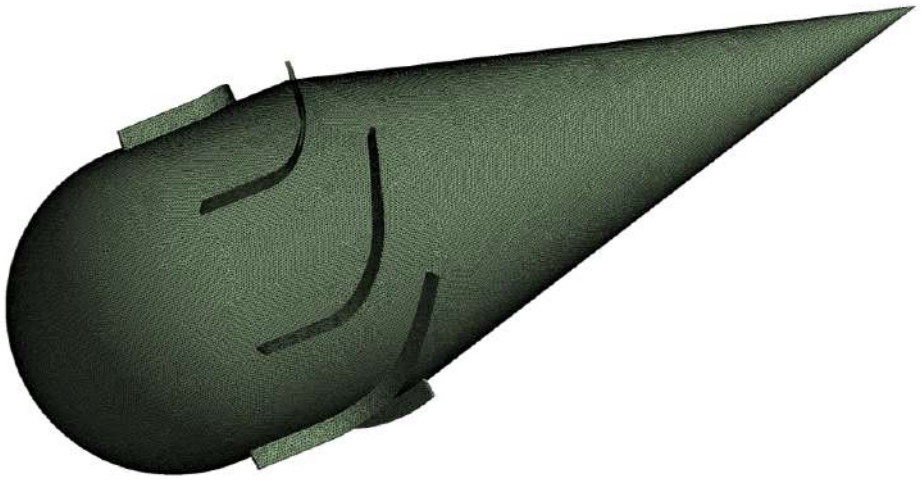

Figure 3. Mesh of swirler

Table 2. Grid Convergence Index for Re = 50. M1, M2 and M3 is the coarse to fine mesh. CN = cells number. RF = refinement factor. Extr. = Richardson Extrapolation.

Mesh	**CN**	**RF**	$W_{blade-out}$	GCI	$U_{blade-out}$	GCI	$\Delta p_{swirler}$	GCI
-	-	-	[m/s]	[%]	[m/s]	[%]	[Pa]	[%]
M1	1,990,651	-	0.002733	-	0.002560	-	0.198016	-
M2	5,172,417	1.37	0.002786	-	0.002641	-	0.204600	-
M3	15,409,880	1.44	0.002820	1.62	0.002682	1.37	0.207773	1,24
Extr.	-	-	**0.002857**	-	**0.002712**	-	**0,209800**	-

The average axial and tangential velocities are calculated at blade trailing edge section as,

$$\bar{V} = \frac{\int_A V dA}{\int_A dA} \tag{7}$$

The pressure drop is defined as pressure difference between average pressure at swirler leading edge section (section-1) and average pressure at swirler trailing edge section (section-2), as

$$p = \bar{p_1} - \bar{p_2} \tag{8}$$

where the average pressure is defined as

$$\bar{p} = \frac{\int_A p dA}{\int_A dA} \tag{9}$$

4. RESULTS AND DISCUSSION

In the present study, the laminar swirling flow induced by static swirler was investigated numerically. The numerical simulations were performed according to Table 1. The results presented in this section were calculated at different dimensionless axial positions (z/D) and radial positions (r/R).

The axial and tangential velocity distribution for Re = 200 are presented in Fig. 4 and 5, for different axial positions starting at cone trailing edge (z/D = 8.8) until nearly end of pipe (z/D = 27.4). The first observation is that the velocity distribution is not symmetrical at positions near close to the swirler. This asymmetrical behavior is due to the vanes (7 vanes) are distributed asymmetrically in the swirler although they are evenly mounted on the hub. Thus, the flow is induced non-symmetrically. The asymmetric distribution can be clearly noted at positions 8.8D and 11.0D. As the flow develops downstream, the flows become approximately symmetrical and this can be noted comparing the axial velocity profile at position 27.4D with theoretical fully develop profile (Figure 4).

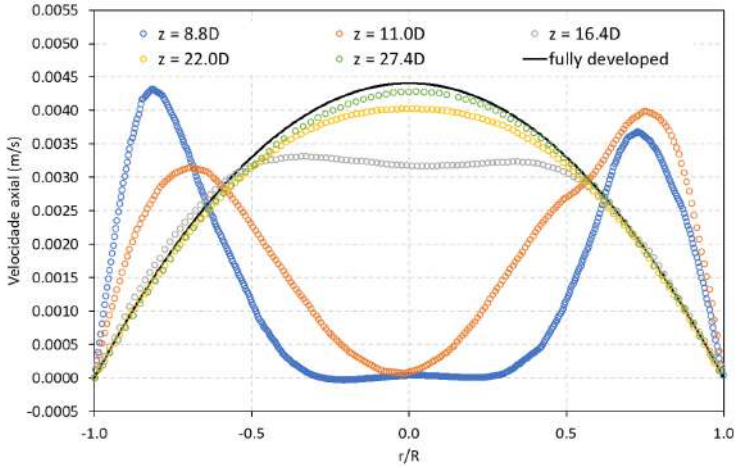

Figure 4. Velocities profiles for Re = 200: Axial velocity.

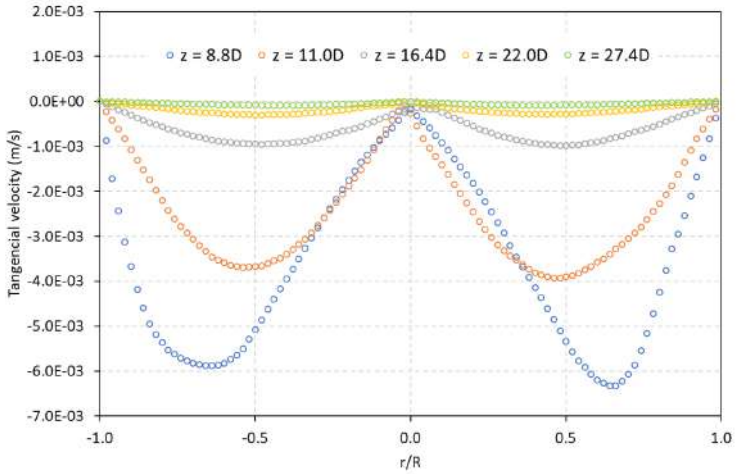

Figure 5. Velocities profiles for Re = 200: Tangential velocity.

Figure 5 shows the distributions of tangential velocity. The results reveal that as the flow develops downstream, the swirl intensity decay until to be approximately zero at the end of pipe. In addition, it is also possible to notice the asymmetry in the velocity distribution, already presented and discussed.

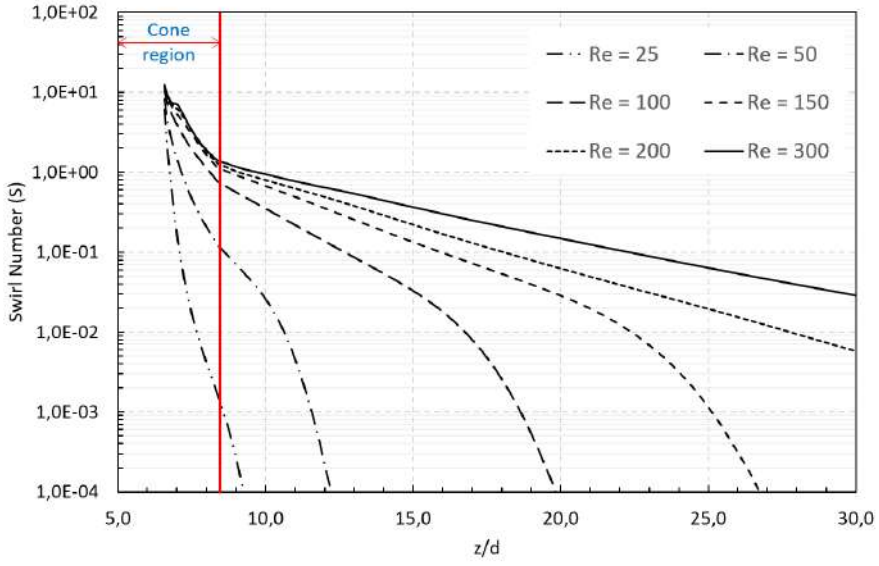

Figure 6. Swirl number for different Reynolds numbers.

The swirl decay for different Reynolds numbers, from the vane trailing edge section to a near outlet pipe region, is shown in Fig. 6. As the swirling flow develops downstream, the wall friction reduces the axial and tangential momentum fluxes in the near wall region thus causing swirl decay. It could be seen from Figure 6 similar behavior for Reynolds number 200 and 300. For theses Reynolds numbers, the swirl decay exponentially towards the downstream with different decay rates at cone region. For lower Reynolds numbers (< 200), the exponential decay is only an approximation. For Re = 25, the swirl number decays rapidly to zero (still in the cone region, approximately) and the tangential velocity is practically zero in this region.

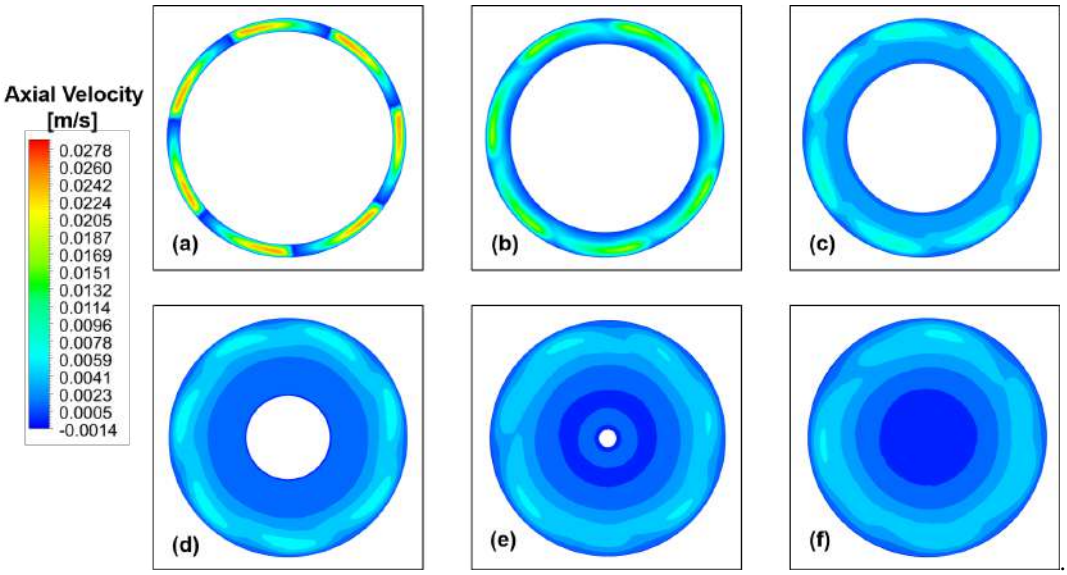

Figure 7. Axial velocity profile for Re=200, for different axial positions: (a) z = 6.6D, (b) 7.1D, (c) 7.7D, (d) 8.2D and (f) z = 9.9D.

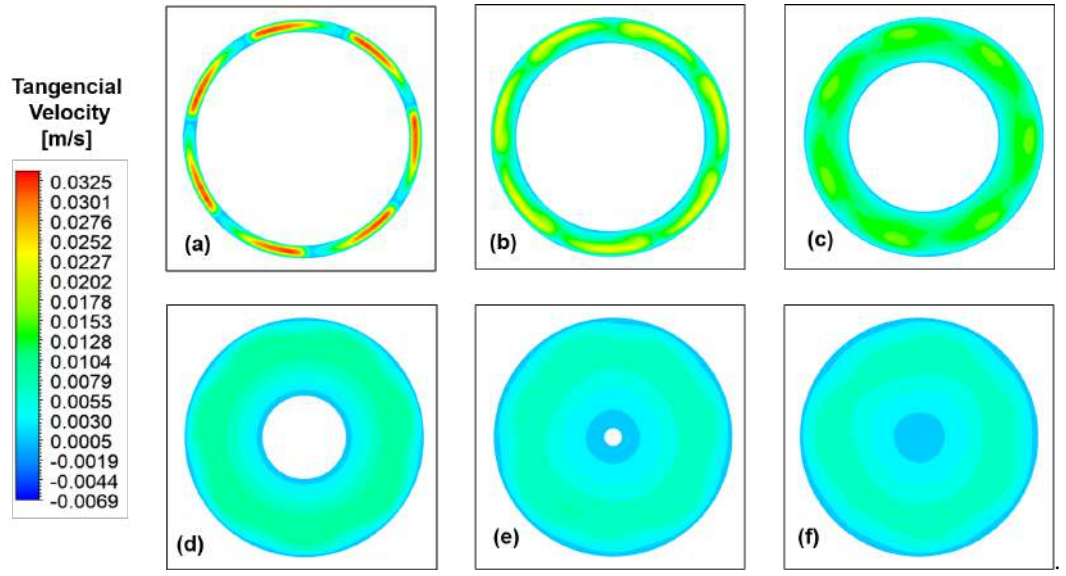

Figure 8. Tangential velocity profile for Re=200, for different axial positions: (a) z = 6.6D, (b) 7.1D, (c) 7.7D, (d) 8.2D and (f) z = 9.9D.

The asymmetry of the as well as the decay of the tangential velocity can also be observed in the Figures 7 and 8 for Re = 200 and six different axial positions (cone region). The flow is deflected by vanes and Figure 7a and 8a shows the axial and tangential velocities at blade outlet (z = 6.6D). Note that the velocity is not constant in the section and the maximum axial and tangential velocities are 0.0278 m/s and 0.0325 m/s respectively. The axial component of velocity is adjusted as the flow develops. Since the cone region is an expansion region (divergent tube type), the axial velocity decreases as shown in the Figures 7b-7f. The decay of tangential velocity in the cone region can also be observed in Fig. 8. At the position 9.9D, the maximum axial and tangential velocities are 0.0008 m/s and 0.01 m/s respectively.

Various streamlines describing the nature of the flow are shown in Fig. 9. The seeding is done at position 6.1D. The

streamlines exhibit helical nature which is common to such kind of flows. As Reynolds numbers increases the swirl also increases since the deflection angle is constant.

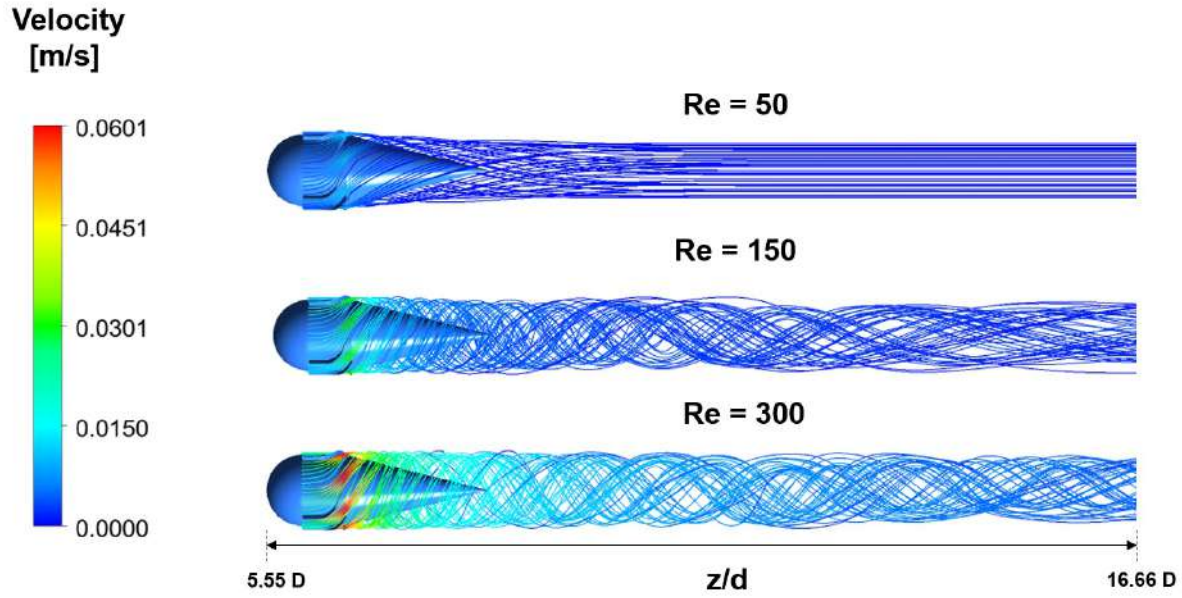

Figure 9. Streamlines for three different Reynolds numbers.

5. CONCLUSIONS

Numerical study of a three-dimensional laminar swirling flow in a pipe induced by static swirler were performed. No considering any numerical approximations for the inlet, the results show that the helical flow is asymmetric, mainly in the region near the swirler. In addition, the results show that swirl decay is only exponential for Re $\geq$ 200. The numerical results confirmed a helical nature to such kind of flows.

6. ACKNOWLEDGMENT

The authors would like to acknowledge CAPES (Coordination for the Improvement of Higher Education Personnel) for Grant and FAPESP (São Paulo Research Foundation) for scientific support 2017/06978-3.

7. REFERENCES

Aksel, M.H. and Kaya, M.T., 1992. "A numerical simulation of the axisymmetric vortex breakdown in a pipe". *Appl. Math. Modelling*.

Ayinde, T.F., 2010. "A generalized relationship for swirl decay in laminar pipe flow". *Sadhana*, Vol. 35, No. 2, pp. 129–137. doi:10.1007/s12046-010-0018-9.

Beaubert, F., Pálsson, H., Lalot, S., Choquet, I. and Bauduin, H., 2016. "Fundamental mode of freely decaying laminar swirling flows". *Aplied Mathematical Modeling*.

Benay, R., 1984. "Numerical modelling of a vortex breakdown in a laminar flow of revolucion". *Rech Aerosp.*

Benim, A.C., Gul, F. and Pasqualotto, E., 2007. "Numerical investigation oh the role of the inlet swirl velocity profile on decay of swirl in pipe flow". *International Conference on Fluid Mechanics and Aerodynamics*.

Bottaro, A., Ryhmingm, I.L., Wehrli, M.B., Rys, F.S. and Rys, P., 1991. "Laminar swirling flow and vortex breakdown in a pipe". *Computer Methods in Applied Mechanics and Engineering*.

Cabral, R.V. and Rocha, A.D., 2017. "Projeto do dispositivo gerador de giro de um hidrociclone axial". *X Simpósio de Iniciação Científica da UFABC*.

Crane, C.M. and Burley, D.M., 1976. "Numerical studies od laminar flow in ducts and pipes". *Journal of Computational and Applied Mathematics*.

Fluent, A., 2019. "Ansys fluent theory guide".

Kiya, M., Fukusako, S. and Arie, M., 1970. "Laminar swirling flow in the entrance region of a circular pipe". *Transactions of the Japan Society of Mechanical Engineers*, Vol. 36, No. 291, pp. 1865–1876. doi:10.1299/kikai1938.36.1865.

Korjack, T.A., 1985. "Numerical studies of laminar flow in ducts and pipes". *Mass Transfer of Decaying Products in Swirling Laminar Pipe Flow*.

Lavan, Z., 1969. "Separation and flow reversal in swirling flows in circular ducts". *Physics of Fluids*, Vol. 12, No. 9, p. 1747. doi:10.1063/1.1692738.

Maynard, A.D., 2000. "A silple model of axial flow cyclone performance under laminar flow conditions". *Journal Aerosol Sci.*

Padmanabhan, N., 1984. "Swirling flow of a fluid in a straight tube". *Indian Journal pure uppl. Math.*

Roache, P.J., 1994. "Perspective: A method for uniform reporting of grid refinement studies". *Journal of Fluids Engineering*, Vol. 116, No. 3, p. 405. doi:10.1115/1.2910291.

Rocha, A.D., Bannwart, A.C. and Ganzarolli, M.M., 2015. "Numerical and experimental study of an axially induced swirling pipe flow". *International Journal of Heat and Fluid Flow*, Vol. 53, pp. 81–90. doi: 10.1016/j.ijheatfluidflow.2015.02.003.

Rocha, A.D., Bannwart, A.C. and Ganzarolli, M.M., 2017. "Effects of inlet boundary conditions in an axial hydrocyclone". *Journal of the Brazilian Society of Mechanical Sciences and Engineering*, Vol. 39, No. 9, pp. 3425–3437. doi:10.1007/s40430-017-0835-4.

Shuja, S., Yilbas, B.S. and Budair, M.O., 2002. "Investigation into a confined laminar swirling jet and entropy production". *International Journal of Numerical Methods for Heat Fluid Flow*.

Silvester, D., Thatcher, R. and Duthie, J., 1984. "The specification and numerical solution of a benchmark swirling laminar flow problem". *Computers & Fluids*, Vol. 12, No. 4, pp. 281–292. doi:10.1016/0045-7930(84)90010-0.

Singh, M.P., Sinha, P.C. and Aggarwal, M., 1980. "Swirling flow in a straight circular pipe". *ZAMM - Zeitschrift für Angewandte Mathematik und Mechanik*, Vol. 60, No. 9, pp. 429–436. doi:10.1002/zamm.19800600908.

Talbot, L., 1951. "Study of laminar swirling pipe flow". *PhD Thesis, University of Michigan.*

Vaidya, H.A., Ertunç, O., Genç, B., Beyer, F., Koksoy, and Delgado, A., 2011. "Numerical simulations of swirling pipe flows-decay of swirl and occurrence of vortex structures". *Journal of Physics: Conference Series, 13th European Turbulence Conference*.

Yao, S. and Fang, T., 2012. "Analytical solution of laminar swirl decay in a straight pipe". *Commun Nonlinear Sci Numer Simulat*.